

Cooperative Converters in Power Electronic Systems

E. Romero-Cadaval, M.I. Milanés-Montero

*R+D Group in Power Electrical and Electronic Systems, University of Extremadura,
Avda. Elvas, s/n, 06006 Badajoz, Spain, e-mail: eromero@unex.es*

ABSTRACT: The specifications of power electronic systems are becoming ever more exigent – better performance (dynamic and steady state), increased efficiency, reliability, and quality, and decreased power rating, size (volume and weight), and cost. One strategy for the overall improvement of these systems is to use various cooperating converters with the system functions being shared among them, optimizing each converter for the functions assigned it. The result will be a converter with better characteristics than a conventional design based on a single converter (or on a simple parallel association of converters) responsible for all the functions assigned to the system. This paper analyzes the possibilities of such cooperative converters, considering the filtering inductor size, and the efficiency, reliability, and power rating.

1 Introduction

The ever more demanding specifications of power electronic systems seek to improve such evaluation indices as:

- Performance, in both steady and transient states.
- Power rating, capable of dealing with higher powers and energies.
- Efficiency, reducing the losses in both passive and active elements.
- Reliability, using modular designs and sometimes redundancy modules.
- Quality, capable of operating with low distortion ratios and a high power factor, even in a disturbed grid.
- Size, low in volume and in weight.
- And above all, with as low a cost as possible.

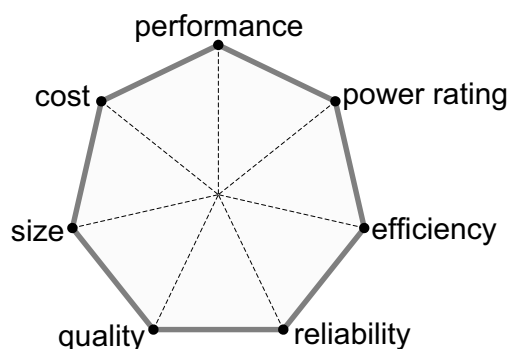


Fig. 1. Ideal shape based on performance indices.

These seven indices of the overall performance of a power electronic system could be represented by the ideal shape shown in Fig. 1, in which each vertex corresponds to the ideal value of the corresponding index.

In [1], a first definition of a multi-converter power electronic system was proposed. The focus of that work, however, was on avoiding the performance degradation or even system destabilization which could arise when the entire system, comprising its various converters, is designed and controlled converter-by-converter based on their stand-alone behaviour.

The cooperative converter concept goes one step further, looking for a compromise solution in which various converters work together for a common purpose or benefit to improve the performance indices overall. It is not just a question of parallelizing converters, but rather one of specializing each converter to optimally achieve a certain partial goal. For example, to attain the ideal shape of Fig. 1, one might use two converters with the shapes shown in Fig. 2, whose joint action will result in a system close to the ideal shape.

Section 2 of this paper describes the essential ideas underlying cooperative converters, and some of the specific objectives to be satisfied by such a system are discussed in Sec. 3. Sections 4 and 5 show how these cooperative converters could improve the system characteristics of two example applications: active power filters, and power injection systems for photovoltaic generation plants. Finally, Sec. 6 presents the conclusions of the study.

2 Cooperative Converters

The use of cooperative converters to obtain optimized power electronic systems has been considered in the literature as an alternative solution for the achievement of one or more design objectives.

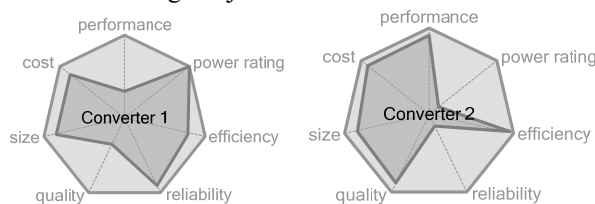


Fig. 2. Ideal shape based on performance indices for a system that uses two cooperative converters.

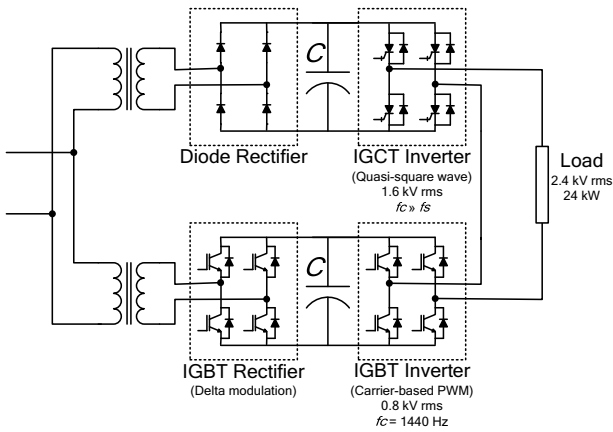


Fig. 3. Single-phase equivalent power circuit of the hybrid multilevel power conversion system [2].

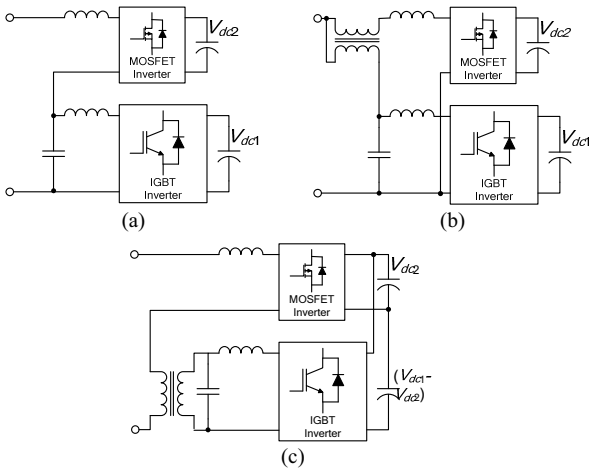


Fig. 4. Single-phase equivalent circuits of series and parallel connected multiconverter active power filter topologies [3]: (a) series-type, (b) parallel-type, and (c) dc-link shared with an low-frequency isolation transformer.

A rectifier topology based on two converters is presented in [2] (Fig. 3). This rectifier operates cooperatively to take advantage of the synergy between the two technologies: latching devices (IGCT) for their high-voltage blocking capability, and non-latching devices (Insulated-gate bipolar transistor, IGBT) for their fast-switching capability. Hence, although the overall device kilovoltampere rating is the same as that of a conventional H-bridge multilevel inverter, one can obtain a significant cost reduction with appropriate selection of the devices. Additionally, employing a hybrid rectifier makes it possible to relieve the grid to a large extent of harmonic interaction.

A similar association of different types of semiconductor converters is applied in [3] (Fig. 4), with the focus of the analysis being the topology of Fig. 4c. The IGBT inverter's function is to support the grid's fundamental voltage and to compensate the fundamental reactive power, and the MOSFET (metal-oxide-semiconductor field-effect transistor) inverter completes the harmonic current compensation. To further reduce the

cost and to simplify the control, the IGBT and MOSFET inverters therefore share the same dc-link at a reduced voltage. In addition, the authors state that the overall noise can be reduced by employing appropriate shielding in the isolation transformer at the output of the high-switching frequency inverter. The proposed active power filter system is inherently more stable than conventional designs, and can adapt to sudden load changes. In the experimental setup, switching frequencies of 3 and 50 kHz were selected to operate the IGBT and MOSFET inverters, respectively. The DC voltage was 450 V for the IGBT inverter and 50 V for the MOSFET inverter.

A cooperative association of converters to drive an induction motor is presented in [4] and [5] (Fig. 5). The topology proposed in [5] comprises a thyristor-based current source inverter, CSI, with a parallel installation of a voltage source inverter, VSI, and the capacitor, which can independently manage the real and the reactive power, with an improved harmonic spectrum. The system can be designed to seek an optimal compromise between the VSI rating and the capacitor size. The collaborative operation of the capacitor allows the VSI load current to be reduced, thereby decreasing the power rating and cost of the VSI. The VSI also works as a harmonic filter, canceling the harmonic current components from the CSI.

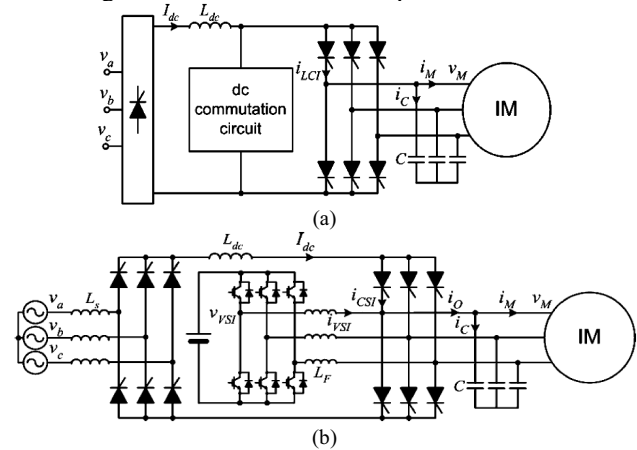


Fig. 5. Drive topologies for an induction motor [5]: (a) conventional drive, (b) cooperative converter topology.

Full compensating systems for distribution networks are introduced in [6]. These are capable of eliminating harmonics, correcting unbalanced loads, and generating or absorbing reactive power. They are based on a combination of a thyristor binary compensator (TBC) and a pulse-width-modulation insulated gate bipolar transistor active power filter (APF) connected in cascade (Fig. 6). The TBC compensates the fundamental reactive power and balances the load connected to the system. The APF eliminates the harmonics and compensates the small amounts of load imbalance or power factor that the TBC cannot eliminate due to its binary condition. The two converters (TBC and APF) work independently, simplifying the control of the system, endowing it with a good dynamic response and greater reliability. It is more economical than other topologies capable of doing the

same work because the high kVAR stage is implemented with thyristors which are cheaper than Gate turn-off thyristors (GTOs). The results show the system to exhibit excellent behaviour under both steady-state and transient conditions.

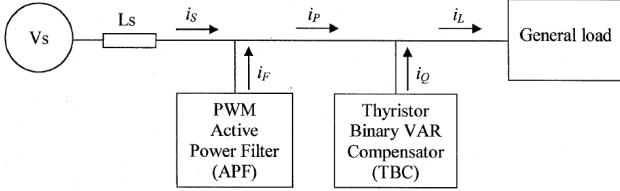


Fig. 6. Combination of a thyristor binary compensator and a PWM-IGBT active power filter [6].

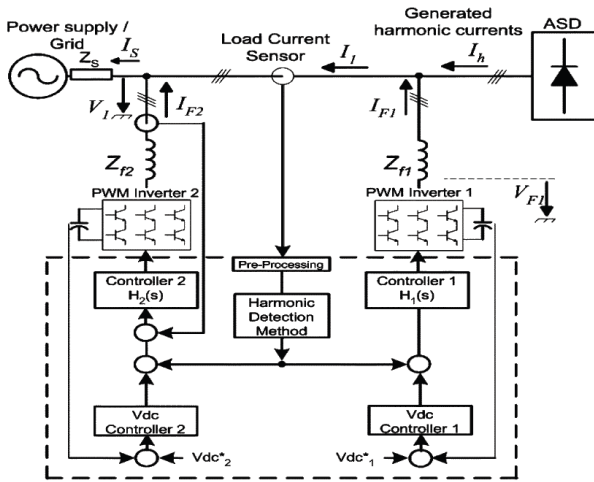


Fig. 7. Simplified diagram of a proposed shunt APF topology with feedback and feedforward loops [7].

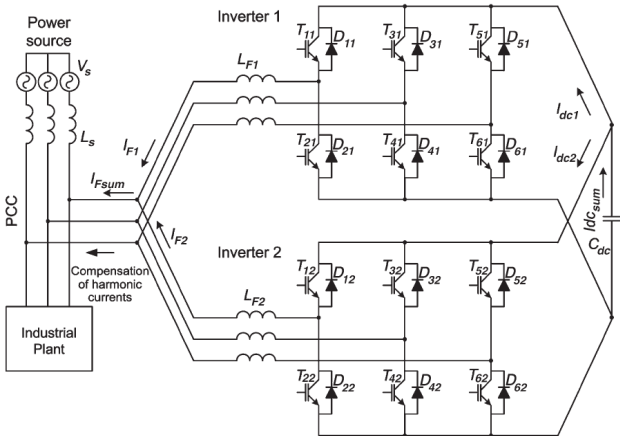


Fig. 8. Diagram of a proposed APF topology with two parallel interleaved inverters sharing the same dc capacitor [8].

Multiple converters (APFs) operating cooperatively are used in [7] to optimize overall performance (Fig. 7). This solution is targeted at medium-power adjustable speed drive applications. One APF is working in feedforward current loop, and the other in feedback current loop. They share the same load current sensor that is located between the points of connection of each inverter to the power system (Fig. 7). The overall system

presents improved stationary performance and dynamic response because each APF is optimally programmed for each state. In sharing the function of load harmonic compensation, the two converters achieve good total harmonic distortion (THD) and current ripple reduction.

A system to compensate the reactive power and current harmonics is presented in [8], comprising two interleaved pulse-width-modulation VSIs connected together to the ac line and sharing the same dc-link capacitor (Fig. 8). Its advantages are: (i) significant reduction in the size of the linkage inductors by decreasing the line-current ripple due to the interleaving; (ii) reduction of the switching stress in the dc-link capacitor due to the shared connection; and (iii) more accurate compensation for high-power applications because the power sharing allows one to use a higher switching frequency in each inverter. The use of smaller line inductors and the replacement of the isolation transformer with common-mode coils reduces costs and allows a faster response in tracking the harmonic-current reference. This, together with the increased reliability due to the topology's characteristic intrinsic modularity, makes it very attractive for high-power industrial APFs.

Another cooperative converter topology for APF applications is discussed in [9] and [10]. The principal focus of the analysis is on the advantages obtained in terms of the filtering inductor sizes and the inverter ratings, making it useful for high power applications. This system will be discussed in detail in Sec. 4.

A cooperative converter for a power injection system (PIS) application for a photovoltaic generation system (PVGS) is presented in [11]. In this case, the PIS consists of two converters: the first is operated with a quasi-square waveform technique, and is responsible for controlling the energy injected into the grid; the second uses a pulse width modulation (PWM) technique and controls the quality of the current waveform. This topology will be discussed in detail in Sec. 5. The possibility of implementing an APF function in addition to that of power injection so as to improve the system's overall capabilities is analyzed in [12].

In sum, therefore, there have been several studies dealing with the association of multiple converters to achieve the same goals as a single converter so as to improve one or more of the evaluation indices. In these systems, known as cooperative converter power electronic systems, each converter is responsible for achieving a selected objective alone or with the aid of another converter in the system.

Sections 4 and 5 will discuss some of the advantages of using cooperative converters in two example applications – APF and PIS.

3 Cooperative converter objectives

This section will present some general considerations about four of the evaluation elements and ratios that can be used to compare a cooperative converter system with the conventional alternative. We shall focus attention on

filtering inductors, converter losses, and reliability issues. Similar analyses could be carried out for other system elements or performance indices.

A. Filtering inductors

Most converters need filtering inductors at their output terminals to control the ripple associated with the switching operation or to mitigate undesired current harmonics.

Either air core or ferromagnetic core inductors can be used, depending on the switching frequency used to operate the power electronic system. Since far less magnetic energy can be stored in an air core, this type of inductor is much larger than its ferromagnetic core autoinductance equivalent. But while they usually have more Joule effect losses, they have neither ferromagnetic losses nor saturation problems.

It might therefore be convenient to associate converters operating at different switching frequencies, so as to be able to use air core inductors in some and ferromagnetic core inductors in others, aiming at a compromise solution that minimizes losses and sizes by taking advantage of the properties of both.

The parameters of these inductors will determine their sizes (volume and weight), and will have to be selected to provide the current derivatives needed for proper power system operation, and to keep the switching ripple below a given limit. Using cooperative converters, one can seek to attain these two objectives independently.

B. Converter losses

The cooperative association of converters with different topologies can reduce converter losses.

For example, the use of a neutral point clamped (NPC) three-level inverter instead of the conventional two-level sinusoidal design reduces total silicon losses per leg by 60% (from 229W to 146W) and module cost by 25% [13] (considering an application of 20 kVA, $V_{LL} = 400$ V, $\cos\varphi = 0.85$, and operating with a switching frequency of 20 kHz).

Typical converter losses for two- or three-level inverter legs that generate sinusoidal currents can be determined using the expressions given by SEMIKRON in [13–15]. These are summarized in Table I.

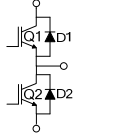
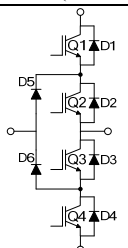
Converter losses also depend on the semiconductor used to implement the converter. A comparative loss analysis of IGBT and GTO is presented in [16].

C. Reliability

Reliability indices can be improved by using cooperative converters constructed with different semiconductor devices [16]. The idea is that one selects the most reliable semiconductor for the converter responsible for the essential functions, and another semiconductor with the desired characteristics (and usually less reliable) to construct the converter that will

assist the first to attain the system objectives. In this way, if one of the cooperative converters fails, which will probably be the less reliable one, the essential functions are guaranteed and only the secondary functions are lost.

Table I. Conduction and switching losses in two- and three-level inverter legs.

	Conduction losses $P_{on} = V_{on} I_{avg} + r_{on} I_{rms}^2$	Switching losses
	 Two-level sinusoidal inverter	
IGBT Q1/Q2	$I_{avg} = i \left(\frac{1}{2\pi} + \frac{m}{8} \cos\varphi \right)$ $I_{rms}^2 = i^2 \left(\frac{1}{8} + \frac{m}{3\pi} \cos\varphi \right)$	$P_{sw} = \frac{1}{\pi} f_{sw} E_{sw} (I_{pk})$
	 Three-level sinusoidal inverter	
IGBT Q1/Q4	$I_{avg} = i \frac{m}{4\pi} [\sin \varphi + (\pi - \varphi) \cos\varphi]$ $I_{rms}^2 = i^2 \frac{m}{4\pi} \left[1 + \frac{4}{3} \cos\varphi + \frac{1}{3} \cos(2\varphi) \right]$	$P_{sw} = \frac{1}{\pi} f_{sw} E_{sw} (I_{pk})$
IGBT Q2/Q3	$I_{avg} = i \left(\frac{1}{\pi} - \frac{m}{4\pi} [\sin \varphi - \varphi \cos\varphi] \right)$ $I_{rms}^2 = i^2 \left(\frac{1}{4} - \frac{m}{4\pi} \left[1 - \frac{4}{3} \cos\varphi + \frac{1}{3} \cos(2\varphi) \right] \right)$	Negligible
Diodes D5/D6	$I_{avg} = i \frac{1}{4} - i^2 \left(\frac{m}{4\pi} \left[\cos\varphi + \frac{2}{\pi} \sin \varphi - \frac{2}{\pi} \cos\varphi \right] \right)$ $I_{rms}^2 = i^2 \frac{1}{4} - i \frac{m}{2\pi} \left[1 + \frac{1}{3} \cos(2\varphi) \right]$	$P_{sw} = \frac{1}{\pi} f_{sw} E_{sw} (I_{pk})$

Indeed, by using cooperative converters, one can operate the essential converter less stressfully in terms of conditions of voltage, current, power, and switching frequency. If the semiconductor is less stressed, its failure rate will be lower.

An example of the reliability analysis of a Medium Voltage Adjustable Frequency Drive (MV-AFD) design utilizing reliability measurement standards is described in [17]. This study uses reliability analysis to compare the two MV-AFD designs shown in Fig. 9 with respect to long life and long service. From the data summarized in the tables of Fig. 10, it was determined that the Mean Time To Fail (MTTF) of the NPC inverter is about 111 hours while that of the cascade H-bridge inverter is about 24.5 hours. The conclusion was that, even with the cell bypass feature of the H-bridge inverter, the reliability of this older design is greatly surpassed by today's modern multilevel inverters for medium voltage applications. In particular, the NPC inverter provides 4.5 times the reliability for roughly the same installed cost, making it currently the only reasonable solution for today's MV-AFD applications.

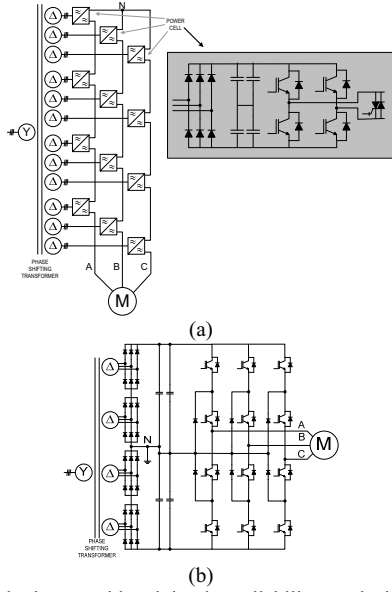


Fig. 9. Topologies considered in the reliability analysis in [17]: (a) cascade H-bridge (Paice) topology, and (b) NPC three-level inverter.

Table 1. NPC Topology.

Component	Quantity	FIT	Total FIT
Diodes	30	100	3000
DC capacitors	4	300	1200
IGBT	12	400	4800
Total			9000

Table 2. H-Bridge Topology.

Component	Quantity	FIT	Total FIT
Diodes	72	100	7200
DC capacitors	72	400	28800
IGBT	48	100	4800
Total			40800

Fig. 10. Data used in the reliability analysis of [17].

D. Power rating

There are constraints on the use of conventional topologies in high power applications due to the limitations of semiconductor technology regarding the inverter rating ([8], [18]). Cooperative converters provide a potential solution to this problem.

For example, the design power rating of the inverter [10] can be calculated as

$$S_{inv} = 3U_{inv}I_{inv}$$

where U_{inv} and I_{inv} are the rms values of the phase-to-neutral voltage and current on the ac side of the inverter. A system based on cooperative converters could be designed so that one of them has high U_{inv} and low I_{inv} values, and the other the opposite, low U_{inv} and high I_{inv} , thereby reducing the overall power rating.

4 Active Power Line Conditioner

In [9] and [10] two cooperative converter based active power line conditioner (APLC) topologies are proposed. The first consists of an association of two conventional active filters, and the second of an association of a conventional active filter with a hybrid active filter.

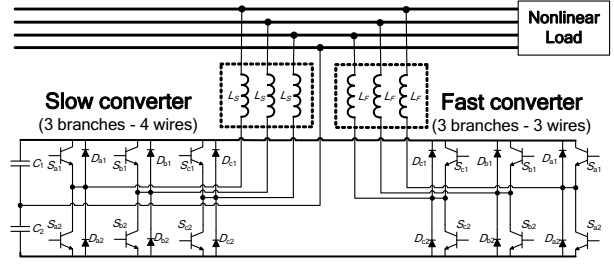


Fig. 11. Proposed APPLC topology.

A. Active power line conditioner based on two cooperative converters

The topology of this power system is shown in Fig. 11. It consists of the parallel association of two VSI inverters. One, denominated the slow converter, has three legs and four wires, and the other, denominated the fast converter, has three legs and three wires. The objective of the overall system is to compensate the reactive power demanded by the load and to cancel the current harmonics this load produces.

To illustrate the operation of the proposed system, a three-phase controlled rectifier with a resistive load will be taken as the nonlinear load. This load demands variable active and reactive power depending on the firing angle. The rectifier's resistive load is set equal to 3Ω to achieve a maximum power consumption of 100 kW (for a firing angle equal to 0°).

The two converters share the system's overall objective cooperatively:

- The slow converter will be responsible for compensating the reactive power, canceling the selected low-order harmonics and maintaining the DC bus voltage.
- The fast converter will be responsible for canceling the high-order current harmonics.

In this case, as will be shown below, the aim of using a cooperative converter is to optimize the filtering inductor (especially in high power applications where this inductor may be large in size). The idea is to use ferromagnetic core inductors (which usually are small in size) in the slow converter, but this can only be done if the switching frequency is low (under 4 kHz).

This is the reason for splitting the current harmonic cancellation between the two converters. The limit order harmonic selected to separate the two parts is the 7th. On the one hand, this selection allows one to attain the objective of reducing the rms value of the fast converter correction current. And on the other, its frequency (350 Hz) is low enough compared with the switching frequency of the slow converter (3 kHz) to result in an appropriate value for the frequency modulation index, which is greater than 9.

The ideal overall reference current, and the currents for each converter in one of the worst cases (a firing angle equal to 30° which produces the maximum instantaneous increment in the load current) are plotted in Fig. 12.

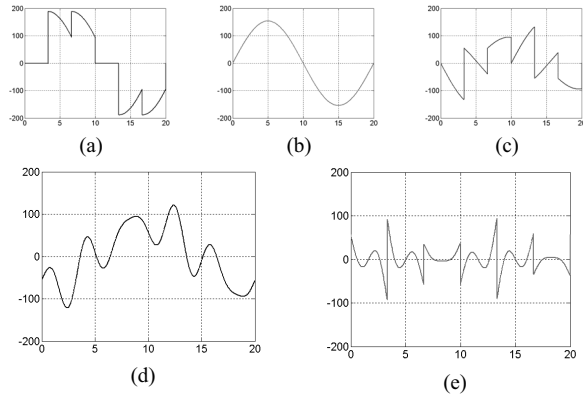


Fig. 12. Current waveforms for a rectifier firing angle of 30° : (a) load current, (b) ideal corrected supply current, (c) total APLC reference current, (d) slow converter reference current, and (e) fast converter reference current.

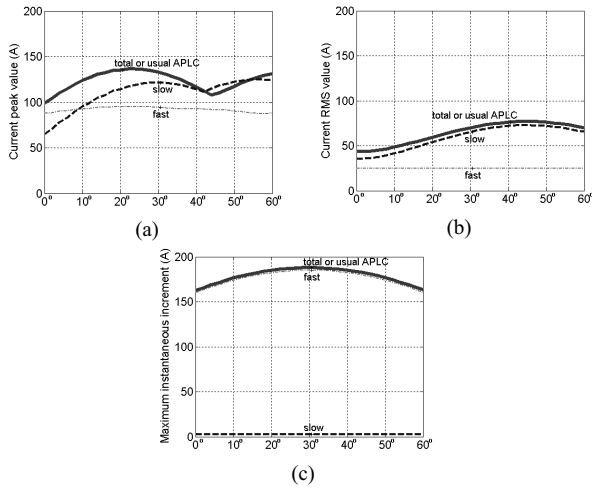


Fig. 13. Converter current characteristics when varying the rectifier firing angle (between 0° and 60°): (a) peak values, (b) rms values, (c) maximum instantaneous increment.

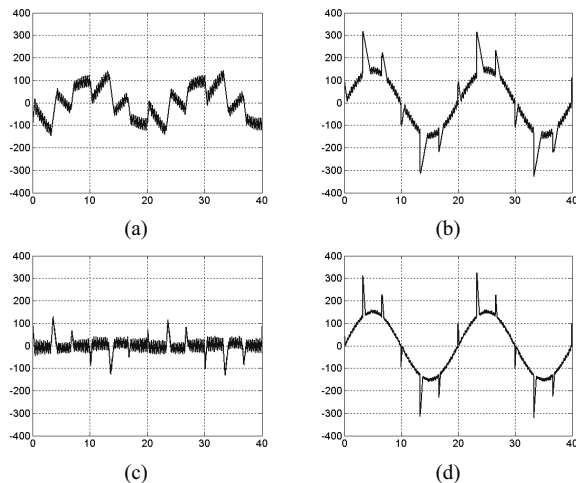


Fig. 14. Relevant current waveforms obtained by simulation for a rectifier firing angle of 30° : (a) slow converter compensating current, (b) load current corrected by the slow converter, (c) fast converter current, and (d) supply current after the correction by the two converters.

This APLC must be able to correct the load current (compensating fundamental reactive power and canceling current harmonic components) for any firing angle of the nonlinear load between 0° and 60° . The main converter current characteristics when varying the rectifier firing angle are shown in Fig. 13. These values have to be taken into consideration in the design of the filtering inductor, and will affect its size (volume, weight, and cost).

In a real implementation, the cooperative algorithm could be changed to simplify the control, avoiding the calculation of current harmonics. The inductance of the slow converter is selected as a compromise value to maintain the ripple of the current after its compensation and to allow a current variation that compensates the high current increment in the load in a given time interval. The fast converter is designed to assist the slow converter when instantaneous current increments occur, and to compensate the switching harmonics produced by the slow converter. The cooperative operation of the two converters is illustrated in Fig. 14. The rms current is 70.6 A and 29.9 A for the slow and fast converters, respectively, values which are close to the ideal (shown in Fig. 13). The converter current peaks are also close to the ideal value (± 100 A), and the slow converter current (Fig. 14a) to the ideal waveform (Fig. 12a).

The parameters of the filtering inductors used for the test in Fig. 14 were 2 mH for the fast converter to control the current ripple to below 10%, and 1 mH for the fast converter to guarantee cooperative operation. The data of these inductors are summarized in Table II.

Total inductor volume is reduced from 3868 to 2913 cm^3 (25%), total weight presents a very small reduction from 22.5 to 22.0 kg (2%), but cost (expressed in kg of Cu and assuming that cost per kg of ferromagnetic normalised U-I core is 1.5/4 times the cost per kg of Cu) is reduced from 22.5 to 13.4 (40%).

Table II. Summary of the most significant filter inductors dimensions: volume, copper wire cross sections, copper weight, iron weight, inductor weight, and cost expressed in kg of cooper.

Filter inductance of ...	V (cm^3)	S _{Cu} mm^2	P _{Cu} kg	P _{Fe} kg	P _{Tot} kg	Cost kg.Cu
A conventional APLC monoconverter	3868	33.2	22.5	-	22.5	22.5
Fast converter of the proposed APLC	685	10.8	3.8	-	3.8	3.8
Slow converter of the proposed APLC	2228	33.2	4.5	13.7	18.2	9.6
Totals for the cooperative converter	2913	-	8.3	13.7	22.0	13.4

B. Active power line conditioner based on the cooperative association of a conventional and a hybrid conditioner.

A cooperative system that associates a conventional APF with a hybrid filter (HF) (Figs. 15 and 16) is presented in [10].

In this topology, the HF is responsible for the fundamental and dominant harmonic components (5th and

7th orders) in the load current, operating at a low switching frequency (slow). The passive filter was tuned to the 5th harmonic component. This device is aided by the fast conditioner, which operates at a higher frequency, compensating the higher harmonic components. The tuned harmonic components left uncompensated by the slow device to avoid passive filter overload and the switching harmonics of the hybrid conditioner are also potential targets for this filter to deal with.

The proposed topology yields a major reduction in the inverter ratings. The ratio of the inverter apparent power to the load apparent power is lower than with conventional APFs and with the topology presented in the previous section which used two cooperative APFs (Table III).

5 Power Injection System

A PIS for a photovoltaic PVGS, that is based on the study of cooperative converters is described in [11], [12], and [19].

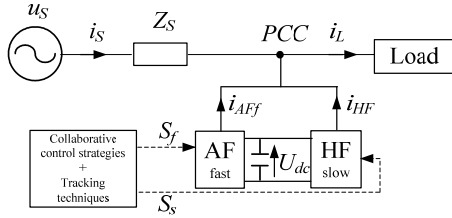


Fig. 15. Block diagram of the parallel-connected multi-converter topology: two power stages (active filter in parallel with a hybrid filter, sharing the dc bus) and one cooperative control stage.

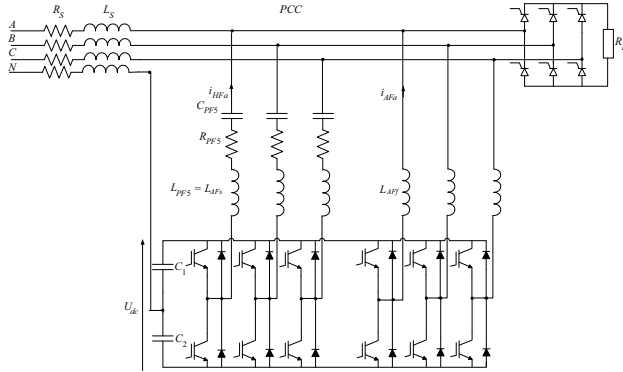


Fig. 16. Three-phase four-wire source with nonlinear load and hybrid multi-converter shunt conditioner.

Table III. Maximum apparent power of the inverter relative to the maximum load power for the worst case firing angle.

	S_{max} (VA)	α	S_{inv} / S_L (%)	
Load	1170.1	0°	-	
Active mono-converter	1067.1	43°	91.2%	
Active multi-converter	<i>AF fast</i>	182.43	44°	15.59%
	<i>AF slow</i>	671.76	43°	57.41%
Hybrid multi-converter	<i>AF fast</i>	182.43	44°	15.59%
	<i>HF slow</i>	247.37	0°	21.14%

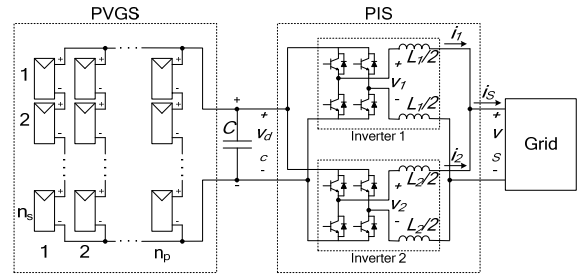


Fig. 17. Scheme of the PIS.

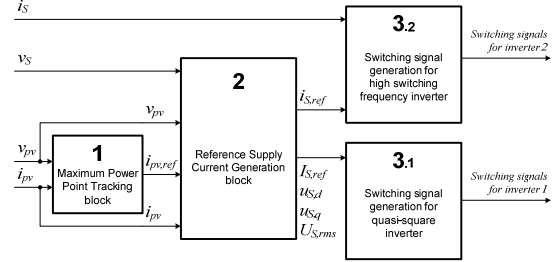


Fig. 18. PIS control scheme.

A single-phase topology (Figs. 17 and 18) is presented in [11]. It is based on the parallel association of two cooperative VSIs: one is operated using a quasi-square voltage waveform strategy (quasi-square waveform inverter, QSWI) and the other operates with a PWM-based strategy (high-switching-frequency inverter, HSFI). The general purpose of the QSWI is to inject the power generated by the PVGS, and that of the HSFI is to be responsible for controlling the quality of the current injected into the grid. One converter operates generating a quasi-square waveform, and the other as a conventional PWM converter, improving the overall quality.

The QSWI inverter generates a current that injects the power extracted from the PVGS (which matches the maximum power) into the grid, but the quality of this current is low (THD>5% and some individual harmonic distortion, IHD_h, above 3%, Fig. 19d [11]).

What actually is the reduction in losses of the proposed system compared with a conventional sinusoidal PWM power injection system? Figure 20 shows plots of the currents that flow through each semiconductor: in a conventional two-level sinusoidal PWM inverter (Fig. 20a), in the QSWI (Fig. 20b), and in the HSFI (Fig. 20c).

If one assumes that the ON-voltage (V_{on}) and ON-resistance (r_{on}) of the IGBT and diodes of the legs are equal, the conduction losses become

$$P_{on} = V_{on} I_{eq,avg} + r_{on} I_{eq,avg}^2$$

where I_{eq} is the equivalent current calculated as the sum of the four devices of each leg (Fig. 20), plotted in Fig. 21 for the three converters involved in the two alternatives being compared. This assumption does not hold in a real device, for example, the SEMIKRON SK30GH123 values for $T_j=125^\circ\text{C}$ are: $V_{on} = V_{CE(sat)} = 3.7$ V and $r_{on} = r_{CE} = 76$ m Ω for the IGBT and $V_{on} = V_F = V_{EC} = 1.8$ V and $r_{on} = r_F = 32$ m Ω for the associated diode [20].

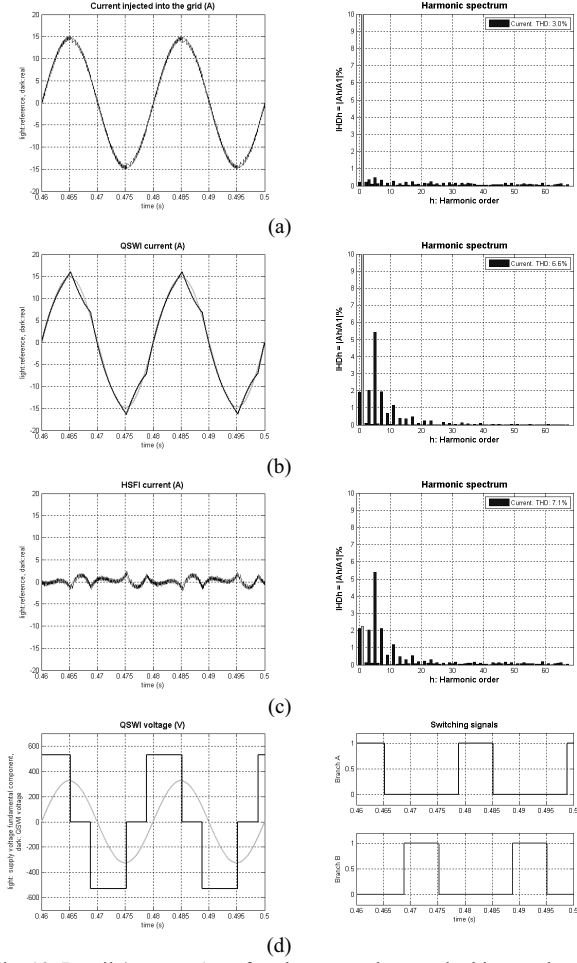


Fig. 19. Detail (near $t = 1$ s, after the system has reached its steady state) of the most representative waveforms for the PIS analysis: (a) total current injected into the grid (sum of the two inverter currents), (b) current generated by the QSWI, (c) current generated by the HSF1, and (d) voltage waveform at the terminal of the QSWI and grid voltage (on the left) and switching signal details (on the right).

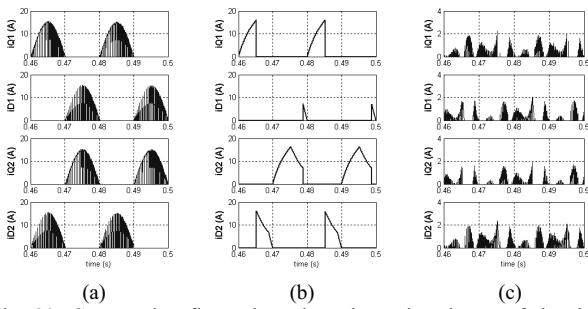


Fig. 20. Current that flows through each semiconductor of the three converters: (a) conventional sinusoidal inverter (Table I), and (b) the QSWI and (c) the HSF1 of the proposed cooperative converter system.

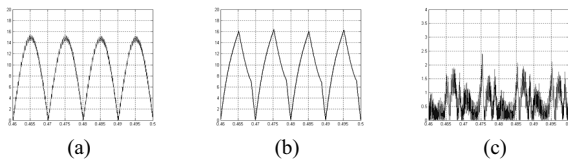


Fig. 21. Equivalent current for each leg of the three converters: (a) conventional sinusoidal inverter, and (b) QSWI and (c) HSF1 of the proposed cooperative converter system.

The switching losses are negligible for the QSWI. For the high switching frequency converters (the conventional sinusoidal inverter and the HSF1 of the cooperative system), one considers the energy losses for ON-commutation (E_{on}) and OFF-commutation (E_{off}) of the IGBT and the diode switching losses (E_{rr}) to be proportional to the instantaneous current value at the switching time. If the switching frequency is high enough, the total switching losses can be calculated by using the average value of the equivalent current, with the expression

$$P_{sw} = (E_{on} + E_{off} + E_{rr}) \frac{I_{eq,avg}}{I_N} f_{sw}$$

where I_N is the nominal current at which E_{on} , E_{off} , and E_{rr} are specified in the manufacturer's semiconductor datasheet. For the previously cited SEMIKRON module, the values of these parameters are $E_{on} = 3.5$ mJ, $E_{off} = 2.5$ mJ, and $E_{rr} = 1$ mJ for a nominal current of 25 A.

The total converter losses, assuming that the currents that flow through all the legs are equal will be given by

$$P_{conv} = n_b (P_{on} + P_{sw})$$

where n_b is the number of legs of the converter (i.e., 2 for all the converters considered).

The relevant equivalent current values and results from applying the above expressions are summarized in Table IV. One may conclude that losses could be reduced by 50% with the use of the proposed system (based on two cooperative converters).

Table IV. Equivalent current values used for the loss calculations, and the resulting losses assuming $V_{on} = 3.7$ V, $r_{on} = 76$ m Ω and $E_{on} + E_{off} + E_{rr} = 7$ mJ, and $f_{sw} = 10$ kHz.

	Conventional	QSWI	HSFI
$I_{eq,avg}$	9.4	9.3	0.7554
$I_{eq,rms}$	10.4	10.3	0.9158
P_{on}	43.1	42.7	2.4
P_{sw}	26.3	0	1.8
n_b	2	2	2
P_{total}	138.8	93.8	8.4

The proposed system is designed to optimize the overall performance at the nominal irradiance level of 1000 W/m². Figure 22 shows a comparison of the evolution of the THD and losses when the irradiance level changes, for the conventional PWM sinusoidal inverter and for the proposed cooperative system. One observes that the proposed topology produces greater losses than the conventional system when the irradiance level is low (below 350 W/m²). In such a case, it might be convenient to turn off the QSWI inverter and let the HSF1 behave as a conventional PWM sinusoidal inverter.

The QSWI is responsible for the essential function of injecting the energy, while the HSF1's function is secondary. Since the essential function does not need fast

switching, some reliable and less stressed semiconductor could be used to improve the reliability of the essential function.

The proposed cooperative converter could also act as an APF [12], compensating the current being demanded by nonlinear loads connected to the same point of the grid as the PIS (Fig. 23).

A single-phase non-controlled rectifier supplying an inductive load is taken as nonlinear load. Figure 24 shows the principal waveforms that describe the PIS+APF operation. In this case the PIS acts as a smart device, not only fulfilling its main objective of injecting the energy generated by the solar cells, but also assisting the grid by controlling the quality of this energy (basically in terms of current THD) and also compensating the poor operation of other loads, ensuring that the total current demanded from the grid has a low distortion. One observes that the current supplied by the PIS is not sinusoidal (Fig. 24b), but is that needed to demand, in conjunction with the nonlinear load, a sinusoidal current from the grid (Fig. 24c). The task of compensating the nonlinear current harmonics is assigned to the HSFI, while the QSWI has the objective of injecting the maximum possible energy from the photovoltaic cells.

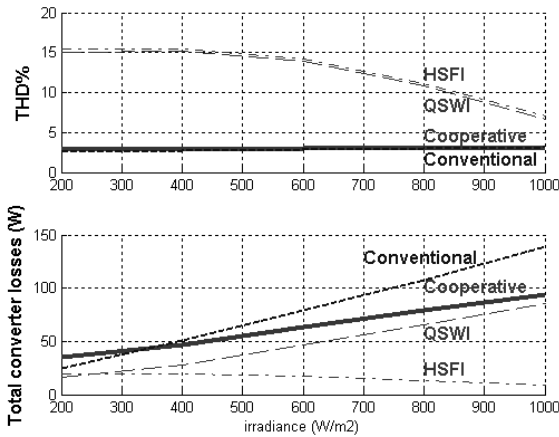


Fig. 22. Comparison of the evolution of the THD and losses associated with the converter analyzed as the solar irradiance varies: (a) THD, (b) total converter losses.

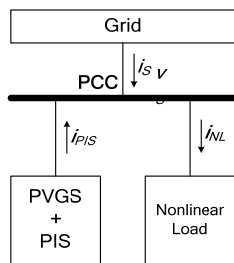


Fig. 23. Connection scheme of the PIS and the nonlinear load to be compensated at the same point of common coupling, PCC.

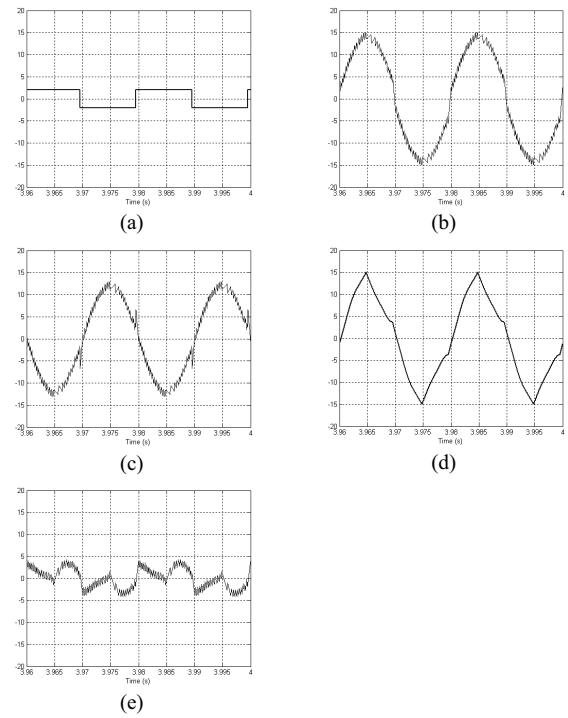


Fig. 24. Principal current waveforms of the PIS+APF cooperative system: (a) nonlinear load current at the same PCC, (b) current injected by the PIS, (c) current demanded from the grid, (d) QSWI current, and (e) HSF current.

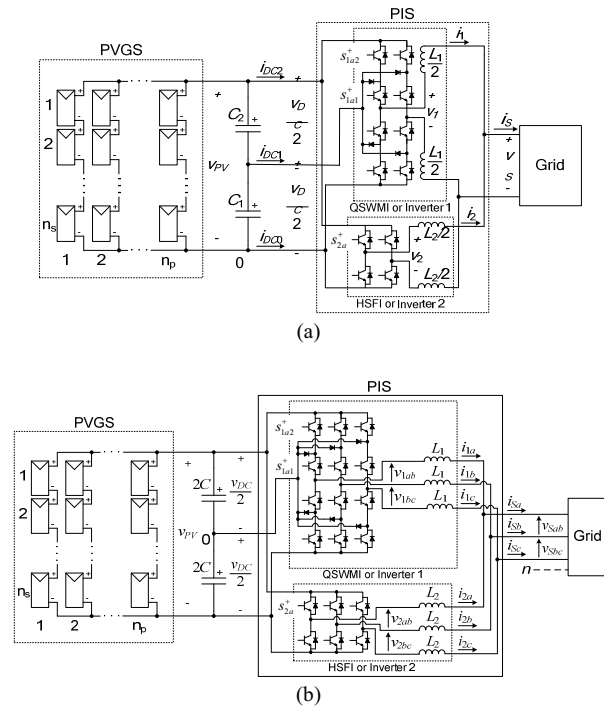


Fig. 25. PIS that uses two cooperative converters: one quasi-square wave inverter with a 3-level neutral point clamped inverter, and a high-switching-frequency conventional inverter: (a) single-phase version, (b) three-phase version.

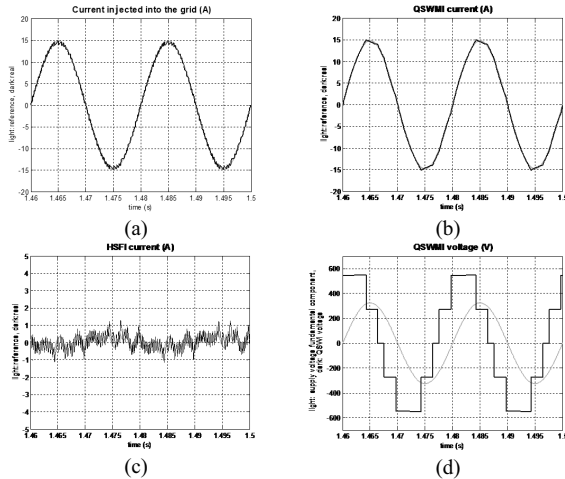


Fig. 26. Detail in the steady state of the most representative PIS waveforms for an irradiance = 800 W/m²: (a) total PIS current, (b) QSWMI (three-level) current, (c) HSFMI (two-level) current, and (d) QSWMI and grid voltages.

Finally the QSWI could be implemented using a three-level neutral point clamped inverter (Quasi-Square-Wave-Multilevel-Inverter, QSWMI, [19], Fig. 25a) with the aim of even further reducing the losses in the two inverters, the QSWMI and the HSFMI. The QSWI topology produces lower losses than the two-level inverter [14], and the HSFMI only has to produce a lower current because the current from the QSWI is closer to the sinusoidal reference. For an irradiance level of 800 W/m², the QSWI gave a current with a THD = 5.1%, and the HSFMI complemented this current to achieve an overall THD = 2.1%. The principal waveforms of the cooperative converter system are plotted in Fig. 26. Finally, a three-phase version of this system is shown in Fig. 25b.

6 Conclusions

Cooperative converters offer an optimizable solution for power electronic systems, allowing the designer to apply reliability principles (some deriving from the fact of parallelizing converters) but going further by improving cost, sizes, and efficiencies.

We have presented some examples, giving a general description of the objectives being sought with these systems, and analyzing in detail two applications – an active filter and a power injection system, focusing on the inductor sizes, inverter ratings, and converter losses, and comparing the results with the corresponding values obtained with a conventional system.

References

- [1] A. Emadi, and M. Ehsani, "Multi-converter power electronic systems: definition and applications". Power Electronics Specialists Conference (PESC 2001, Vancouver, Canada, June 2001), pp. 1230-1236.
- [2] M.D. Manjrekar, P.K. Steimer, and T.A. Lipo, "Hybrid Multilevel Power Conversion System: A Competitive Solution for High-Power Applications". IEEE Transactions on Industry Applications, vol. 36, no. 3, pp. 834-841, 2000.

- [3] S. Kim, and P.N. Enjeti, "A New Hybrid Active Power Filter (APF) Topology". IEEE Transactions on Power Electronics, vol. 17, no. 1, pp. 48-54, 2002.
- [4] S. Kwak, H.A. Toliyat, "Multilevel Converter Topology Using Two Types of Current-Source Inverters". IEEE Transactions on Industry Applications, vol. 42, no. 6, pp. 1558-1564, 2006.
- [5] S. Kwak, T. Kim, "An Integrated Current Source Inverter With Reactive and Harmonic Power Compensators". IEEE Transactions on Power Electronics, vol. 24, no. 2, pp. 348-357, 2009.
- [6] J. Dixon, Y. del Valle, M. Orchard, M. Ortúzar, L. Morán and C. Maffrand, "A Full Compensating System for General Loads, Based on a Combination of Thyristor Binary Compensator and a PWM-IGBT Active Power Filter", IEEE Trans. Industrial Electronics, vol. 50, no. 5, pp. 982-989, 2003.
- [7] L. Asiminoaei, C. Lascu, F. Blaabjerg, I. Boldea, "Performance Improvement of Shunt Active Power Filter With Dual Parallel Topology". IEEE Transactions on Power Electronics, vol. 22, no. 1, pp. 247-259, 2007.
- [8] L. Asiminoaei, E. Aeloiza, P. N. Enjeti, and F. Blaabjerg, "Shunt Active-Power-Filter Topology Based on Parallel Interleaved Inverters", IEEE Trans. Industrial Electronics, vol. 55, no. 3, pp. 1175-1189, 2008.
- [9] E.R. Cadaval, F.B. González, M.I.M. Montero, "Active power line conditioner based on two parallel converters topology". Compatibility in Power Electronics (CPE'05, Gdynia, Poland, June 2005), pp. 134-140.
- [10] M.I.M. Montero, E.R. Cadaval, F.B. González, "Hybrid Power Line Conditioner Based on Two Parallel Converters Topology". Przegląd Elektrotechniczny Electrical Review, no. 10, pp. 66-72, 2007.
- [11] E. Romero-Cadaval, M.I. Milanés-Montero, E. González-Romera, F. Barrero-González, "Power Injection System for Grid-Connected Photovoltaic Generation Systems Based on Two Collaborative Voltage Source Inverters". IEEE Transactions on Industrial Electronics, vol. 56, no. 11, pp. 4389-4398, 2009.
- [12] E. Romero-Cadaval, M.I. Milanés-Montero, F. Barrero-González, E. González-Romera, "Power injection system for photovoltaic generation plants with active filtering capability". Compatibility and Power Electronics (CPE'09, Badajoz, Spain, May 2009), pp. 35-42.
- [13] R. Ramin, M. Di-Lella, "SEMISTOP® 3-level inverter for UPS". Presentation. (Available in <http://www.semikron.com>, accessed in April 2010).
- [14] M. Di-Lella, R. Ramin, "IGBTs for 3-level inverters. Improved efficiency in DC/AC conversion". Bodo's Power Electronics in Motion and Conversion. September 2008, pp. 22-24. (Available in <http://www.semikron.com>, accessed in April 2010).
- [15] Semikron application manual. Web-document. (Available in <http://www.semikron.com>, accessed in April 2010).
- [16] S. Bernet, R. Teichmann, A. Zuckerberger, and P. Steimer, P., "Comparison of High Power IGBTs and Hard Driven GTOs for High Power Inverters", Applied Power Electronics Conference and Exposition (APEC '98, California, USA, February 1998), pp. 711-718.
- [17] EATON White Paper TD02000001E, "The Reliability of Neutral Point Clamped vs. Cascaded H-Bridge Inverters", October 2009, available in <http://www.eaton.com>, accessed in May 2010.
- [18] S. Bhattacharya, P.-T. Cheng and D. Divan, "Hybrid Solutions for Improving Passive Filter Performance in High Power Applications". IEEE Transactions on Industry Applications, vol. 33, no. 3, pp. 732-747, 1997.
- [19] V.M. Miñambres-Marcos, E. Romero-Cadaval, M.I. Milanés-Montero, M.A. Guerrero-Martínez, F. Barrero-González, P. González-Castrillo, "Power Injection System for Photovoltaic Plants based on a Multiconverter Topology with DC-Link Capacitor Voltage Balancing". International Conference on Power Electronics and Electrical Engineering (OPTIM 2010, Brasov, Romania, May 2010).
- [20] SEMIKON SK 30GH123 datasheet (http://www.semikron.com/products/data/cur/assets/SK_30_GH_123_24605701.pdf), accessed in April 2010.